SMAR 2019 – Fifth Conference on Smart Monitoring,
Assessment and Rehabilitation of Civil Structures

SMAR 2019

A simplified model for the shear strength in RC and PC beams, and for punching shear in slabs, without or with shear reinforcement, including steel, FRP and SMA

Antoni CLADERA [1], Antonio MARÍ [2], Carlos RIBAS [1], Eva OLLER [2], Jesús M. BAIRAN [2], Noemí DUARTE [2], Raul MENDUIÑA [2]

[1] University of Balearic Islands, Palma, Spain

[2] Universitat Politecnica de Catalunya, Barcelona, Spain

Contact e-mail: antoni.cladera@uib.es

ABSTRACT: Shear in beams and punching shear in slabs, is a long-time hot topic for design and safety evaluation. Due to the brittle behavior in shear of the reinforced concrete (RC) and prestressed concrete (PC) members, the assessment of existing structures must be carried out using reliable models, and, if possible, models based in the mechanical principia, in order to clarify the physics behind the failure for practicing engineers.

In this communication, a simplified model for shear in beams and punching shear in slabs will be summarized. The same mechanical model, originally derived for concrete beams reinforced with fiber reinforced polymers (FRP) longitudinal and/or transversal reinforcement, has been extended to many different particular cases, following always the basic mechanical principia usually considered in structural engineering. The model can be currently applied for two way slabs, one-way slabs and reinforced concrete or prestressed beams. For beams, the case of slender and non-slender beams may be solved in a continuous way, including the possibility of considering the different behavior of beams with rectangular, T- or I- cross section, or different shear reinforcement materials, such as steel, FRP or shape memory alloys (SMA).

The shear strength predicted by the proposed simplified equations has been compared with the experimental results of 2399 tests and with the predictions by the Eurocode 2 and a more general background model also derived by the authors.

1 INTRODUCTION

Shear strength verification and design of concrete members is still an intensive research topic. When a reinforced or prestressed concrete element is subjected to a combination of shear and flexure, diagonal cracks appear and multi-axial stress states take place in regions that exhibit a markedly complex behavior, resulting the so-called shear resisting actions. These shear resisting actions contribute to the shear force transfer between the two portions of the element at each side of the crack. It is well-accepted that the following shear resisting actions exist (ASCE- ACI Committee-445, 1998): shear resisted in the un-cracked compression chord, shear transferred in the cracked zone of the web by means of aggregate interlock and residual tensile stresses, dowel action of the longitudinal reinforcement and the truss action requiring transversal reinforcement.

The mechanics of the previous actions are very diverse and exhibit complex interactions among them; hence development of a universally accepted formulation to account for shear forces has

not been achieved yet and it is necessary to take important assumptions to derive compact expressions. In this paper, a brief description of the Multi-Action Shear Model (Marí, Bairán, *et al.*, 2015) and its simplification, the Compression Chord Capacity Model (Cladera *et al.*, 2016), is made, explaining how the models incorporate the contributions of the different shear transfer mechanisms. For beams, the case of slender and non-slender beams may be solved in a continuous way, including the possibility of considering the different behavior of beams with rectangular, T- or I- cross section, or different shear reinforcement materials, such as steel, FRP or SMA. The model can be also applied for two way slabs, as will be presented during next sections. Note that this communication presents, for the first time, the complete set of simplified equations that may be used in many different practical situations.

2 GENERAL OVERVIEW OF THE MULTI-ACTION SHEAR MODEL (MASM)

It is generally agreed that as the load increases in a RC member failing in shear, damage concentrates around a critical shear crack, originally a flexural crack, which arrives to the neighborhood of the flexural neutral axis (Fig. 1), this is usually called the first branch of the crack. Under incremental loading, a second branch of the crack develops inside the un-cracked concrete chord, which will connect the first branch of the crack and the load application point, producing failure. The main assumption of the MASM, backed by the empirical observation of many authors (Zararis and Papadakis, 2001; Carmona *et al.*, 2007; Yu *et al.*, 2016), is that when the second branch of the critical crack develops, the load does not significantly increase, as softening of the concrete in the compression zone initiates. During the crack propagation inside the flexural compression zone, redistribution of internal forces may occur, affecting the relative importance of the different shear resisting actions.

To associate the initiation of the shear failure to the propagation of the second branch of the critical crack results in a significant simplification of the problem, since it allows formulating a failure criterion expressed in terms of concrete stresses in the compression chord (Kupfer's biaxial failure envelope). This failure criterion depends on the compression and tensile strength of concrete, which have less scatter than other parameters needed in kinematical criteria.

Therefore, the Multi-Action Shear Model, based on classic mechanics, proposes explicit equations for the different shear transfer actions considering that the tip of the shear critical crack has propagated until the flexural neutral axis. The shear strength, V_u in Eq. (1), is the sum of the shear resisted by the transverse reinforcement, if it exists, V_s, and by the shear resisted in the un-cracked compression chord, V_c, the shear transferred across web cracks, V_w, and the dowel action in the longitudinal reinforcement, V_l, see Fig. 2. The shear strength must be lower than the shear force that produce failure in the concrete struts, $V_{u,max}$, in Eq. (2). See Table 1 for the dimensionless equations governing each contributing component. See reference (Cladera *et al.*, 2016) for further information related to these equations, factors, and parameters.

$$V_u = \left(V_c + V_w + V_l\right) + V_s = f_{ctm} \cdot b \cdot d \cdot \left(v_c + v_w + v_l\right) + v_s \cdot f_{ctm} \cdot b \cdot d \tag{1}$$

$$V_{u,\max} = \alpha_{cw} b_w z v_1 f_{cm} \frac{\cot\theta}{1+\cot^2\theta} \tag{2}$$

Strut crushing, Eq. (2), may occur in cases when a large contribution of V_s exists, so this check is necessary. For this cases, the authors have adopted the formulation of current EC-2 (European Committee for Standardization, 2002), derived from plasticity models, but assuming that the angle of the compression strut is equal to the angle of the critical crack.

Table 1. Summary of dimensionless shear contributing components.

Shear resisting action	Dimensionless equations	
Compression chord	$v_c = \zeta\left[\left(0.88 + \left(0.20 + 0.50\frac{b}{b_w}\right)v_s\right)\frac{x}{d} + 0.02\right]\frac{b_{v,eff}}{b}K_p$	(3)
Cracked concrete web	$v_w = 167\frac{f_{ctm}}{E_{cm}}\frac{b_w}{b}\left(1 + \frac{2G_f E_{cm}}{f_{ctm}^2 d_0}\right)$	(4)
Longitudinal reinforcement	$if\ v_s > 0 \rightarrow v_l = 0.23\frac{\alpha_e \cdot \rho_l}{1 - x/d}$	(5a)
	$if\ v_s = 0 \rightarrow v_l = 0$	(5b)
Shear reinforcement	$v_s = (d_s - x)\cot\theta\frac{A_{sw}\cdot f_{yw}}{s\cdot f_{ctm}\cdot b\cdot d} \approx \frac{0.85 d_s A_{sw}\cdot f_{yw}}{s\cdot f_{ctm}\cdot b\cdot d}$	(6)

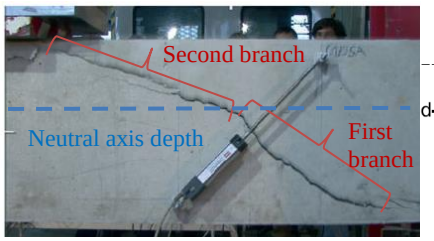

Figure 1. Critical shear crack evolution.

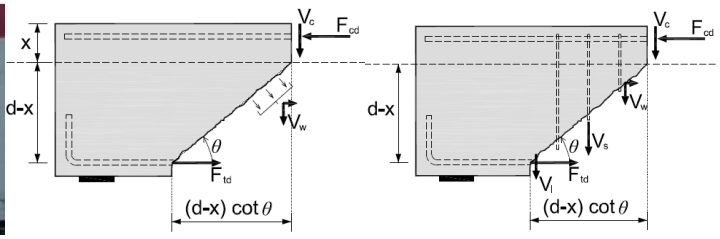

Figure 2. MASM contributing actions at failure.

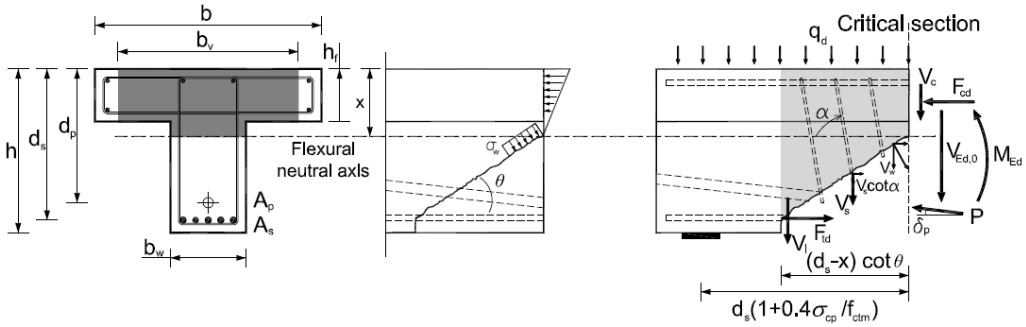

Figure 3. Contributing actions for a T beam and notation.

3 THE COMPRESSION CHORD CAPACITY MODEL (CCCM)

The previously presented model, the MASM, with explicit equations for each shear resisting action may result too complex for daily engineering practice. For this reason, a transparent simplification was carried out (Cladera *et al.*, 2016), with the main premise that the shear transferred by the compression chord is the main resisting action in the considered failure state. To derive the more compact expression, v_w (Eq 4) and v_l (Eq. 5) have been incorporated into v_c (Eq. 3) with constant average values, and the equations have been reformatted.

The main equations governing the shear strength for the CCCM are presented in Table 2, where x/d is the relative neutral axis depth and it is equal to x_0/d for RC members without axial loads (Eq. 12). The relative neutral axis depth may be simplified as proposed by the expression at right hand in Eq. (12). The effective flanges width for shear strength (Figure 3) is given by $b_{v,eff}$ (see Eq. 13), being b_w the web width. For the determination of f_{cd} in Eq. (9), f_{ck} shall not be taken greater than 60 MPa. This limitation is provided due to the larger observed variability in shear strength of members with higher strength concrete. Finally, d_0 is equal to the effective depth of the cross-section, d, but not less than 100 mm.

For members with small depth and not heavily reinforced in bending, i.e. some one-way slabs without shear reinforcement, the shear transferred by residual tensile stresses across the critical shear crack is probably comparable to the shear transferred by the uncracked concrete in the compression zone. However, the equation for the nominal shear strength provided by concrete,

Table 2. Summary of the CCCM equations.

Equations	Expressions	
Shear strength	$V_{Rd} = V_{cu} + V_{su} \leq V_{Rd,max}$	(7)
Strut crushing	$V_{Rd,max} = \alpha_{cw} b_w z \nu_1 f_{cd} \frac{cot\theta + cot\alpha}{1+cot^2\theta}$	(8)
Concrete contribution	$V_{cu} = 0.3\zeta \frac{x}{d} f_{cd}^{2/3} b_{v,eff} d \not< V_{cu,min} = 0.25 \left(\zeta K_c + \frac{20}{d_0}\right) f_{cd}^{2/3} b_w d$	(9)
Shear reinforcement	$V_{su} = 1.4 \frac{A_{sw}}{s} f_{ywd} (d_s - x) sin\alpha \ (\cot\theta + \cot\alpha)$	(10)
Factors	**Expressions**	
Size and slenderness effect	$\zeta = \frac{2}{\sqrt{1+\frac{d_0}{200}}} \left(\frac{d}{a}\right)^{0.2} \not< 0.45$	(11)
Relative neutral axis depth	$\frac{x_0}{d} = \alpha_e \rho_l \left(-1 + \sqrt{1 + \frac{2}{\alpha_e \rho_l}}\right) \approx 0.75(\alpha_e \rho_l)^{1/3}$	(12)
Effective flanges width	$if\ x \leq h_f \rightarrow\ b_{v,eff} = b_v = b_w + 2h_f \leq b$	(13a)
	$if\ x > h_f \rightarrow\ b_{v,eff} \approx b_w + (b_v - b_w) \left(\frac{h_f}{x}\right)^{3/2}$	(13b)
Crack inclination	$\cot\theta = \frac{0.85 d_s}{d_s - x} \leq 2.5$	(14)

expression on the left in Eq. 9, was derived from the MASM assuming that the shear transferred in the compression zone was the predominant transfer action. For this reason, a minimum value for the shear strength provided by concrete, $V_{cu,min}$, is defined (on the right in Eq. 9), with the assumption that the residual tensile stresses that crosses the first branch are significant and that the contribution on the compression zone must be limited.

The shear resisted due to the shear reinforcement is given by Eq. 10. The constant 1.4 in Eq. 10 is not a calibration factor, but a term to take into account the confinement of the concrete in the compression chord caused by the stirrups (Cladera *et al.*, 2016). The previous equation is equivalent to consider the vertical force of the stirrups intersected by the first branch of the critical crack. The crack inclination, θ, is an important parameter in the shear strength (Eq. 14). Based on experimental observations made by the authors and summarized in (Cladera *et al.*, 2015; Marí, Bairán, *et al.*, 2015), the horizontal projection of the first branch of the flexural-shear critical crack is considered to be equal to $0.85d_s$, where d_s is the distance between the maximum compressed concrete fiber and the centroid of the mild steel tensile reinforcement.

3.1 Effects of prestressing in the shear strength

In partially prestressed members, in which flexural cracks may develop at service under certain load combinations, a shear-flexure failure mechanism may take place, as it occurs in many RC members. In such cases the crack inclination, the neutral axis depth, the stress levels, and, consequently, the shear transferred by the uncracked concrete chord and by the stirrups, are affected by the level of the prestressing force (Marí *et al.*, 2016). In a simplified way, to apply the CCCM for prestressed or axially loaded members subjected to compression, the neutral axis depth can be estimated in a simplified manner by means of Eq. 15, which represents an interpolation between x=x_0 and x=h for a fully prestressed section (decompression). Note that the increase of the neutral axis depth depends on the ratio $\frac{\sigma_{cp}}{\sigma_{cp}+f_{ctm}}$ and not only on σ_{cp}.

$$N_{Ed} \geq 0 \ \rightarrow \ \ x = x_0 + 0.80(h - x_0) \left(\frac{d}{h}\right) \frac{\sigma_{cp}}{\sigma_{cp}+f_{ctm}} \leq h \tag{15}$$

Taking into account the neutral axis depth given by Eq. 15, it is possible to apply all the other Equations given in Table 2 to obtain the shear strength of members subjected to compression.

Some heavily prestressed concrete members may be uncracked in bending. In this case, the previously presented models (MASM and CCCM) are not valid, as the main assumption of the

initial bending crack would be incorrect. For prestressed members without stirrups and no flexural cracking, the derivation of a design expression according to Mohr's circle of stresses assuming Kupfer's biaxial failure surface as failure criteria is carried out in (Marí *et al.*, 2016). In the case of PC members with shear reinforcement, once the web cracks, the stirrups start working and a shear force higher than the cracking shear can be resisted. For this reason, in PC members with shear reinforcement, it is assumed that MASM and CCCM may always be used.

3.2 Effects of tensile forces in the shear strength

Tensile forces reduce the neutral axis depth. A parametrical study using a non-linear numerical model considering tension stiffening was carried out to study the variation of the neutral axis depth for tensile loads and the concomitant bending moment, resulting in Eq. (16). Note that, for this case, it is necessary to explicitly take into account the concomitant bending moment, and, therefore, for predicting the shear strength the procedure requires performing iterations, but the model is straightforward for design purposes.

$$N_{Ed} < 0 \;\rightarrow\; x = x_0 \left(1 + 0.1 \frac{N_{Ed} d_s}{M_{Ed}}\right) \geq 0 \tag{16}$$

The shear strength will depend on the ratio N_{Ed}/M_{Ed}, and therefore, it will not be affected by the load partial factors. In contrast, the shear strength in current EC-2 depends on N_{Ed}, and the shear strength is reduced when the load partial factors are applied to the axial tensile force.

3.3 Non-slender beams

Non-slender beams are considered those in which *a/d* is less than 2.5 (Fig. 4). This situation takes place in deep beams or in slender beams when there are point loads applied near the supports. The model has been recently extended for this situation, although it has not been yet published. Non-slender beams show higher shear strength than slender beams. This is considered in the proposed model through the following differential aspects of the observed structural behavior: a) the different position and inclination of the critical crack, which runs straight from the inner ends of the bearing and loading plates, resulting in a value cot $\theta = a/d$. Such value increments the size and slenderness effect factor, Eq. 11, of the model, which is proportional to $(d/a)^{0.2}$; b) the influence of the vertical stresses produced by the loading plate, on the stress state in the critical point of the un-cracked concrete chord. Such confining stresses increment the shear capacity of the compression chord; c) the effects of the disturbed distribution of strains and stresses when loads are applied close to the support, which modifies the neutral axis depth compared to a slender beam. Moreover, in non-slender beams, the use of horizontal reinforcement distributed along the web is very common to control the crack widths, and this reinforcement has been also considered. The equations given in Table 2 are valid in this case, substituting Eqs. (9)-(10) by (17)-(20).

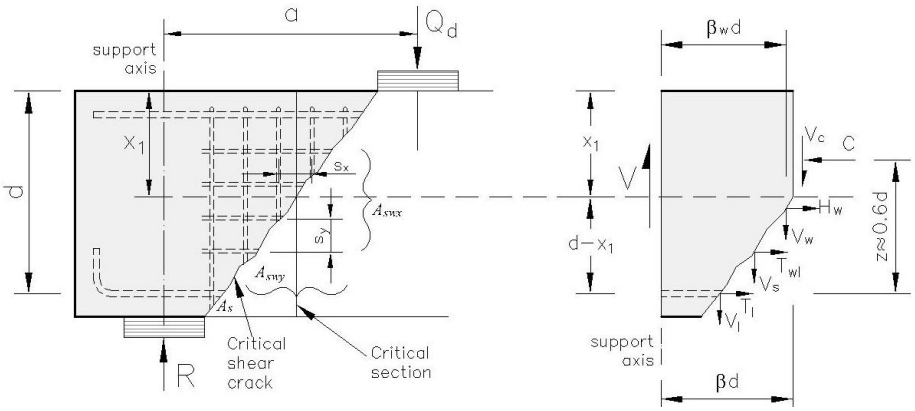

Figure 4. Non-slender beam: notation and forces acting on the free body part of the beam.

$$V_{cu} = 0.3\,\xi\frac{x}{d}K_{ad}f_{cm}^{2/3}bd \quad (17)$$

$$V_{su} = V_{swy} + V_{swx} \quad (18)$$

$$V_{swy} = \frac{A_{swy}}{s_x}(d - x_1)\cot\theta\,\sigma_{swy} \quad (19)$$

$$V_{swx} = 0.5\,\frac{A_{swx}}{s_y}(d - x_1)\tan\theta\,\sigma_{swx} \quad (20)$$

where $K_{ad}=1+(2.5-a/d)^2$. The stress at the vertical stirrups, σ_{swy}, and at the longitudinal flexural reinforcement, σ_{swx}, may be lower than the yielding stress at ULS, and may be obtained:

$$\sigma_{swx} = \frac{f_{ctm}\,K_{ad}}{\rho_l}\frac{x_1}{d}cot\theta \le f_{yw} \quad (21)$$

$$\sigma_{swy} = \frac{f_{ctm}\,K_{ad}}{\rho_l}\frac{x_1}{d}cot^3\theta \le f_{yw} \quad (22)$$

where $\rho_l=A_s/bd$. In order to account for the increment of the neutral axis depth, a parabolic variation of x is assumed between a/d =2.5 ($x_1=x$, B-region) and a/d=0 ($x_1=d$) resulting:

$$\frac{c_1}{d} = \frac{c}{d} + (1 - \frac{c}{d})(1 - 0.4\frac{a}{d})^2 \le 1 \quad (23)$$

3.4 FRP reinforced concrete members

The extension of the CCCM for its use in FRP-RC members without stirrups was carried out at (Marí, Cladera, Ribas, *et al.*, 2018), altogether with the extension for Steel Fibre Reinforced Concrete Beams (not included in this communication). The modulus of elasticity of the FRP bars is taken into account in the model through the neutral axis depth x/d, which is a function of the ratios between the modulus of elasticity of the reinforcement (steel or FRP) and that of the concrete. In addition, crack widths are bigger than in identical steel reinforced concrete beams, thus reducing the aggregate interlock and the residual tensile stresses transferred along the crack. Consequently, the minimum shear $V_{cu,min}$ of Eq (9) is not meaningful for FRP reinforced beams. For the same reinforcement ratio and applied bending moment, compressive concrete stresses are higher in FRP-RC beams than in steel RC beams, and the assumption of linear concrete behavior in compression may deviate from the actual behavior. Therefore, the neutral axis depth computed by means of Eq. (12), is lower than the actual one, and the shear stress that may be resisted by the compressive chord is higher as compressive stresses are higher. These two effects compensate, and Eq. (9) continues to be valid (disregarding $V_{cu,\,min}$ as already stated).

As no yielding takes place in the FRP bars, the maximum bending moment of an FRP reinforced section will be that producing a concrete compressive strain $\varepsilon_c=\varepsilon_{cu}\approx0.004$. For this purpose, when calculating the shear strength, it should be verified that a brittle flexural failure does not occur before reaching the shear strength given by Eq. (9).

For beams with FRP stirrups, their contribution can be considered according to (Oller *et al.*, 2015).

4 PUNCHING SHEAR FOR RC SLABS

A punching strength mechanical model, based on the beam shear model previously presented, were published at (Marí, Cladera, Oller, *et al.*, 2018), considering:

- The distribution of radial bending moments in a slab supported on isolated columns, different from those produced in cantilever beams: the critical crack in a slab is partially developed inside a D (discontinuity) region: the critical crack develops directly to the intersection between the column face and the compressed slab face.
- According to the adopted failure criterion, the critical perimeter is the perimeter where the critical crack reaches the un-cracked compressed zone. Therefore, its distance to the column face depends on the span length, on the load level, on the longitudinal reinforcement ratio, and

on the cracking moment per unit length. Its value ranges from 0.4d to 0.7d, so for simplicity reasons a reasonable value of 0.5d is adopted.

- Due to the proximity of the critical perimeter to the column face, the confining vertical stresses introduced by the column affect the state of stresses at the critical point where failure initiates, thus enhancing the shear capacity of the slab.
- The tangential bending moments around the column produce compressive stresses that also confine the concrete compression chord of the slab. Such confinement in the tangential direction increases the concrete compression strength in the radial direction, affecting the Kupfer's biaxial failure envelope in the compression-tension branch and enhancing the concrete chord capacity to withstand shear stresses.
- The efficiency of the shear reinforcement depends on its position and anchorage capacity. An expression for the maximum stress that the reinforcement may develop before losing its anchor capacity, based on bond, was presented at (Marí, Cladera, Oller, *et al.*, 2018).

The full set of equations may not be reproduced here for respecting the maximum length of the communication, but they may be found at (Marí, Cladera, Oller, *et al.*, 2018).

5 VERIFICATION OF THE PROPOSED MODEL AND CONCLUSIONS

The comparison between the predicted shear strength by the CCCM, MASM and EC-2 and the experimental shear strength measured in 2399 tested members is presented in Table 3. The information is presented separately for 10 different previously published shear-databases. For the different studied cases, the coefficients of variation of the V_{test}/V_{pred} ratio computed using the CCCM or MASM are lower than for the Eurocode-2 predictions. The comparison of the predictions by CCCM and EC2 for the four initial databases included in Table 3 (RC and PC slender beams) is also graphically presented in Figure 5. The CCCM has also been satisfactorily used for critical shear beams externally strengthened using Shape Memory Alloys (Rius *et al.*, 2019), although the comparison is not shown here for brevity.

This communication has presented, for the first time, the complete set of the CCCM equations that may be used in many different practical situations, showing the advantages of using a solid mechanical model. The model was derived with clearly formulated assumptions, allowing their review when necessary for many different cases.

Table 3. Verification of the proposed model: mean value and COV(%) for V_{test}/V_{pred} ratio.

Database	# tests	CCCM		MASM		Eurocode 2	
		Mean	COV	Mean	COV	Mean	COV
RC slender beams without shear reinforcement	784	1.17	18.5	1.04	18.9	1.10	27.9
RC slender beams with shear reinforcement	170	1.16	14.1	1.05	17.0	1.47	26.4
PC slender beams without shear reinforcement	214	1.18	16.5	1.02	19.6	1.56	29.8
PC slender beams with shear reinforcement	117	1.17	18.6	1.05	15.1	1.54	37.2
RC non-slender beams without web reinforcement	153	1.35	26.7	-	-	1.70	28.2
RC non-slender beams with vertical web reinforcement	171	1.25	19.3	-	-	2.41	74.0
RC-non slender beams with vert. and horiz. web reinf.	86	1.28	22.3	-	-	2.94	88.3
RC slender beams reinf. with FRP bars w/o stirrups	144	1.16	16.9	1.09	14.9	-	-
Slabs without shear reinforcement	328	1.19	15.1	-	-	1.17	17.6
Slabs with shear reinforcement	232	1.17	14.9	-	-	1.07	17.9

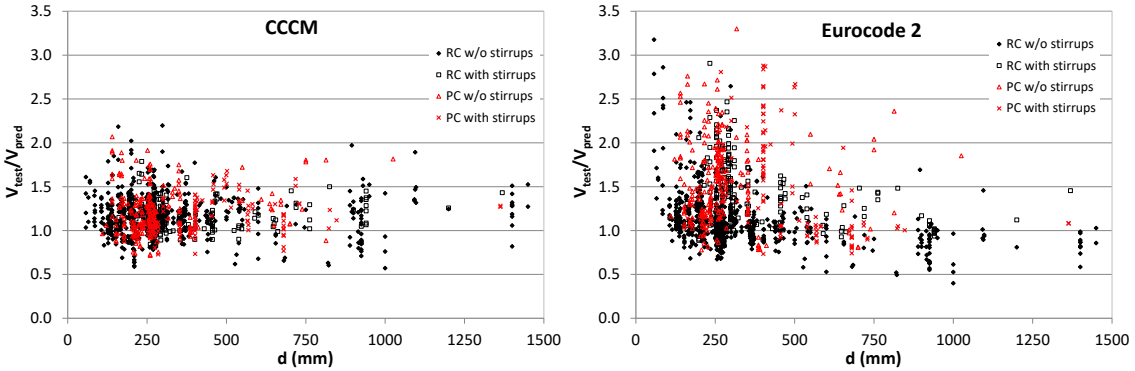

Figure 5. Correlation between the predictions and the experimental results for 4 studied databases.

6 ACKNOWLEDGEMENTS

This communication was developed in the framework of the project HORVITAL BIA2015-64672-C4-3-R and BIA2015-64672-C4-3-R (AEI – FEDER, UE).

7 REFERENCES

ASCE-American Concrete Institute (ACI) Committee-445 (1998) 'Recent approaches to shear design of structural concrete', *Journal of Structural Engineering*, 124(2), pp. 1375–1417.

Carmona, J. R., Ruiz, G. and del Viso, J. R. (2007) 'Mixed-mode crack propagation through reinforced concrete', *Engineering Fracture Mechanics*, 74(17), pp. 2788–2809.

Cladera, A., Marí, A., Bairán, J. M., Ribas, C., Oller, E. and Duarte, N. (2016) 'The compression chord capacity model for the shear design and assessment of reinforced and prestressed concrete beams', *Structural Concrete*, 17(6), pp. 1017–1032. doi: 10.1002/suco.201500214.

Cladera, A., Marí, A., Ribas, C., Bairán García, J. M. and Oller, E. (2015) 'Predicting the shear-flexural strength of slender reinforced concrete T and I shaped beams', *Engineering Structures*, 101, pp. 386–398.

European Committee for Standardization (2002) *Eurocode 2: Design of Concrete Structures: Part 1: General Rules and Rules for Buildings*. European Committee for Standardization.

Marí, A., Bairán, J., Cladera, A., Oller, E. and Ribas, C. (2015) 'Shear-flexural strength mechanical model for the design and assessment of reinforced concrete beams', *Struct. Infrastr. Eng.* 11(11), pp. 1399–1419.

Marí, A., Bairán, J. M., Cladera, A. and Oller, E. (2016) 'Shear design and assessment of reinforced and prestressed concrete beams based on a mechanical model', *Journal of Structural Engineering*, 142(10).

Marí, A., Cladera, A., Bairán García, J. M., Oller, E. and Ribas, C. (2015) 'Shear-flexural strength mechanical model for the design and assessment of reinforced concrete beams subjected to point or distributed loads', *Structure and Infrastructure Engineering*, 8(4), pp. 337–353.

Marí, A., Cladera, A., Oller, E. and Bairán, J. M. (2018) 'A punching shear mechanical model for reinforced concrete flat slabs with and without shear reinforcement', *Engineering Structures*, 166, pp. 413–426.

Marí, A., Cladera, A., Ribas, C., Oller, E. and Bairán, J. (2018) 'Simplified Multi-Action Shear Model for Plain or Steel Fibre Reinforced Concrete Beams Longitudinally Reinforced with Steel or FRP Bars', in *Towards a rational understanding of shear in beams and slabs - fib Bulletin 85*, pp. 260–273.

Oller, E., Marí, A., Bairán, J. M. and Cladera, A. (2015) 'Shear design of reinforced concrete beams with FRP longitudinal and transverse reinforcement', *Composites Part B: Engineering*, 74.

Rius, J. M., Cladera, A., Ribas, C. and Mas, B. (2019) 'Shear strengthening of reinforced concrete beams using shape memory alloys', *Construction and Building Materials*, 200, pp. 420–435.

Yu, Q., Le, J.-L., Hubler, M. H., Wendner, R., Cusatis, G. and Bažant, Z. P. (2016) 'Comparison of main models for size effect on shear strength of reinforced and prestressed concrete beams', *Structural Concrete*. Ernst & Sohn, 17(5), pp. 778–789.

Zararis, P. D. and Papadakis, G. C. (2001) 'Diagonal shear failure and size effect in RC beams without web reinforcement', *Journal of Structural Engineering*, 127(7), pp. 733–742.